Effect of Antimony Addition on Characteristics of Melt - Spun Pb - Sn Alloy

F.Abd El-Salam, M.T.Mostafa, R.H.Nada and A.M.Abd El-Khalek

Physics Dept., Faculty of Education, Ain Shams University, Cairo, Egypt.

The effect of antimony additions on the characteristics of melt-spun Pb-12 wt.%Sn alloy was investigated. The dynamic resonance technique was applied to study the internal friction, Young`s modulus and thermal diffusivity. Also, the dependence of specific heat under constant pressure on Sb content was studied. Isothermal resistivity changes were used to trace the discontinuous precipitation in the studied alloys. It was suggested that inhibited boundary movement caused by Sb segregation at the sweeping reaction fronts retard and ultimately terminate the discontinuous precipitation process. Marked effect was observed with lower Sb addition. X-rays and differential thermal analysis were used to identify structure variations as bases to explain the observed results.

Introduction

Rapid solidification by melt-spinning or chill-block casting technique produces continuous splat-quenched solid tapes. The resulting tapes are particularly suitable for investigating the mechanical properties of splat-quenched alloys by conventional tensile testing. In such technique, the cooling rate is reasonably uniform so that the microstructure shows less variability [1].

The process of rapid solidification improves the mechanical properties [2-6] and leads to the formation of new intermediate phases [7], amorphous and fine microstructures [8-10] extended solubility [11], anomalous vacancy concentrations [12] or suppression of martensite formation [13]. In Pb-Sn alloy, calculations [14] showed that thermo-solute convection in the dendrites zone during solidification can produce heavily localized inhomogeneties in the composition of the final alloy.

In Pb-Sn alloys directionally solidified in a positive thermal gradient, macrosegregation along the length of the sample takes place [15]. Pb-Sn eutetic alloy was examined and reported by many authors to show outstanding superplasticity [16-18]. It was found [19] that pre-stressing the rapidly solidified Pb-Sn-Sb-Ag alloys deteriorated their elastic, inelastic and electric behaviour. Pb-Sn is one of the earliest and most well documented systems for the discontinuous precipitation (DP) process [20] which is deleterious to the mechanical, physical and chemical properties of alloys.

Creep characteristics in Pb-10wt. % Sn alloy were investigated [21, 22]. The marked increase of the transient creep parameters observed above 413 K was attributed to the thermal dissolution of Sn-rich phase in Pb-rich phase [21]. Also, the increase in the strain sensitivity parameter with increasing the deformation temperature was attributed to the diffusion process which enhances cross-slip and climb of dislocations [22]. In the same alloy, the work-hardening parameters decreased, depending on the existing amount of the second phase and its corresponding diffusivity within the matrix [23].

Microadditions of Cu, up to 2.5 wt.%, to Sn-Sb-Ag ternary bearing alloys and rapid quenching from the melt, were found [24] to cause marked changes in the elastic stiffness and finer-grained structures.

Electrical resistivity variations in Pb-Sn soldering alloy during solidification were used to estimate the solid mass fraction as a function of temperature [25]. Electrical resistivity of melt-spun Pb-Sn alloys, showed strong dependence on macroadditions [26]. It was suggested that alloying additions may interface with nucleation event by changing the precipitate characteristics and /or boundary properties [20].

The present study aims at investigating the effect of temperature and ternary addition on the structural, mechanical and electrical properties of the

melt-spun Pb-12wt.%Sn alloy. It is also aimed at studying the discontinuous precipitation (DP) process in the binary and ternary alloys.

Experimental Procedure

Pb-12 wt.%Sn and $PbSn_{12}Sb_x$ alloys with x = 0, 0.5, 1, 1.5, 2 and 2.5 wt.%Sb were prepared from high purity Pb, Sn and Sb (99.99%). The materials in the proper ratio were melted in a pyrex tube for 1h. The melt was rapidly solidified by using a single roller type melt-spinning technique [3]. The sample edges were treated to suit the different intended measurements. The microstructure of the different samples was identified by using X-rays Philips diffractometer, model PW 1050/70, with Cu-K_α radiation of wavelength 0.1542 nm.

Measurements of internal friction Q^{-1}, dynamic elastic modulus Y and thermal diffusivity D_{th} were carried out by applying the dynamic resonance technique. This method is based mainly on the theory of free vibrations of solid bodies [27]. Full details of the experimental arrangement and procedure have been published elsewhere [26]. The resonant frequency F_o and the full width at half-maximum amplitude ΔF obtained from the resonant curve are used to calculate Q^{-1}, Y and D_{th} as follows [28]:

$$\mathbf{Q^{-1}} = \frac{\mathbf{\Delta F}}{\sqrt{\mathbf{3}}\,\mathbf{F_o}} = \mathbf{0.5773 \tan \delta} \qquad (1)$$

Where **tan δ** is the mechanical loss $\frac{\mathbf{\Delta F}}{\mathbf{F_o}}$,

$$\mathbf{D_{th}} = \frac{\mathbf{2\,t^2 F_o}}{\boldsymbol{\pi}} \qquad (2)$$

Where t is the thickness of the sample, and

$$\left(\frac{\mathbf{Y}}{\mathbf{d}}\right)^{1/2} \frac{\mathbf{K}}{\mathbf{2\pi}} = \frac{\mathbf{L^2 F_o}}{\mathbf{Z^2 t}} \qquad (3)$$

where **d** is the density of the sample under test, **L** is the length of the vibrating part of the sample, **K** is the radius of gyration and **Z** is a constant depending on the mode of resonance. For the fundamental mode of resonance **Z** assumes [29] the value 1.875.

The electrical resistance was measured by using Kelvin double bridge model Misr Fatramo 1830 suitable for use in the range from 0.2 μΩ to 11 Ω with maximum current 10 A. Immediately after solidification the specimen was transferred to a water bath kept at constant precipitation temperature T_p

controlled within ± 0.5K in the range from 298K to 328K in steps of 5K. After any precipitation time t_p, the instantaneous resistance R_t was recorded to calculate the fractional change in resistivity,

$$\frac{\Delta R}{R_o} = \frac{R_t - R_o}{R_o} \qquad (4)$$

where $\mathbf{R_o = R_t}$ at $\mathbf{t_p = 0}$.

The values of $\mathbf{R_t}$ were monitored till $\mathbf{R_t = R_f}$ when $\mathbf{(dR_t/dt_p) \leq 0.04\ (dR_t/dt_p)_{max}}$ so that $\mathbf{R_f}$ signifies the practical end of the discontinuous precipitation (DP) process [20].

Results and Discussion

Fig.1 shows the resonant curves for all the tested samples. The Sb concentration dependence of Y, Q^{-1} and D_{th} is given in Fig. (2 a, b and c), respectively.

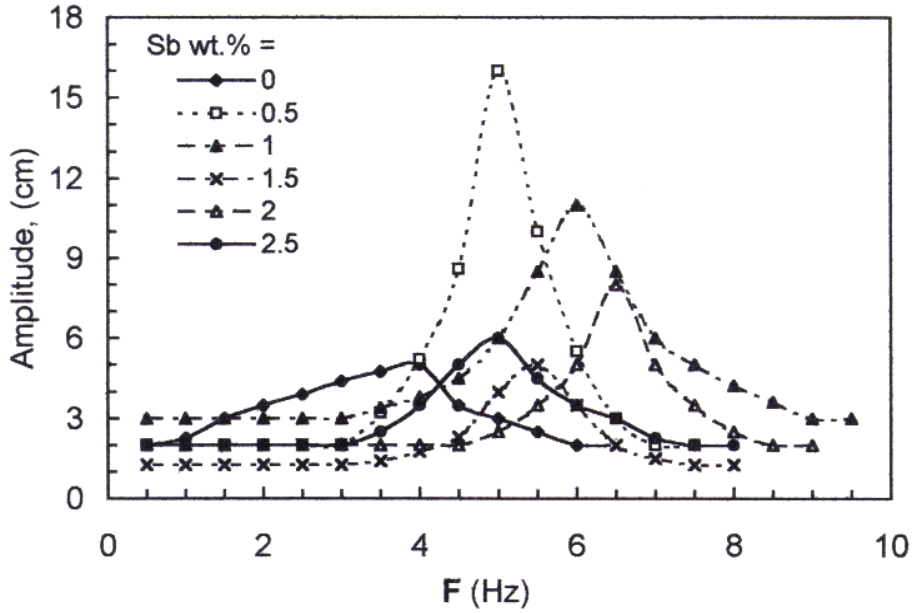

Fig. (1): Resonance curves for binary (Pb Sn_{12}) and the ternary tested alloys with different Sb wt.% additions.

The increase of Y with increasing Sb content Fig.(2a) might be due to the local elastic strains induced by the dispersed solute atoms in the α- (Pb) matrix, which hinder the motion of dislocations [30]. In Fig.(2b), Q^{-1} increased with

adding 0.5wt%Sb and further increase of Sb content decreased it. The increased Sb content makes the alloy brittle and harder. This decreases the density of mobile dislocations and consequently the mechanical loss. The variation of D_{th} as a function of Sb content shown in Fig. (2c) might be a result of the dependence of the mode of distribution of Sn and Sb atoms in the α (Pb) matrix on the added amount of Sb. Fig.(3a) shows the thermograms of the binary and ternary alloys obtained in the temperature range from 20°C (293 K) to 500°C (773 K) with a heating rate of 10°C /min. The melting endotherms vary from 523K to 563K with increasing Sb content. The temperature variations of the endset (liquidus, T_L) and the onset (solidus, T_S) with increasing Sb content are given in Fig.(3b). The observed variations are quite sensitive to composition variations. Although both T_L and T_S in general, decreased with increasing Sb content, T_S showed an increase at 0.5 wt.%Sb and T_L increased at 2.5 wt.%Sb.

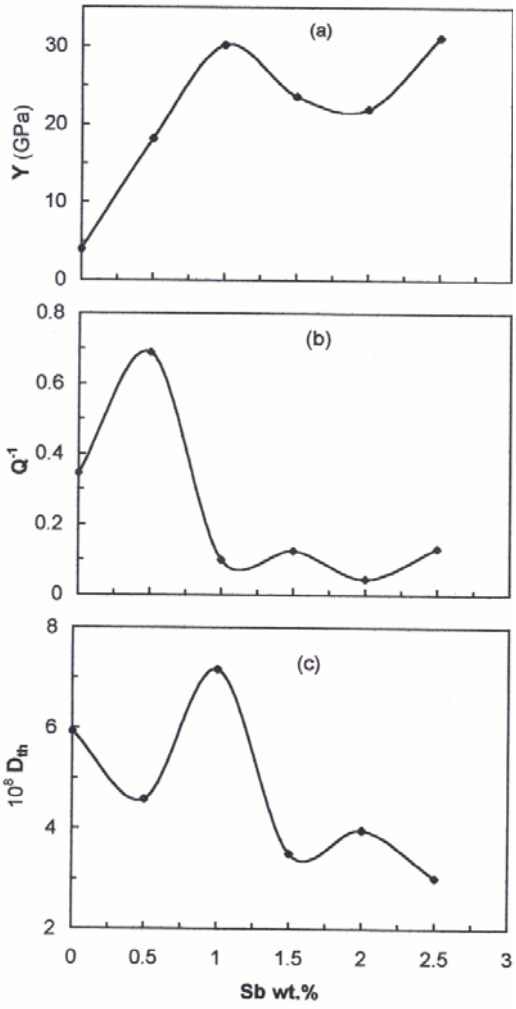

Fig. 2: The Sb concentration dependence of :
a) dynamic elastic modulus Y ,
b) internal friction Q^{-1} ,
c) thermal diffusivity D_{th}.

The temperature dependence of C_p shown in Fig.4a has peak values $(C_p)_{max}$ at temperatures depending on Sb content. The dependence of $(C_p)_{max}$ on Sb content is given in Fig.(4b).

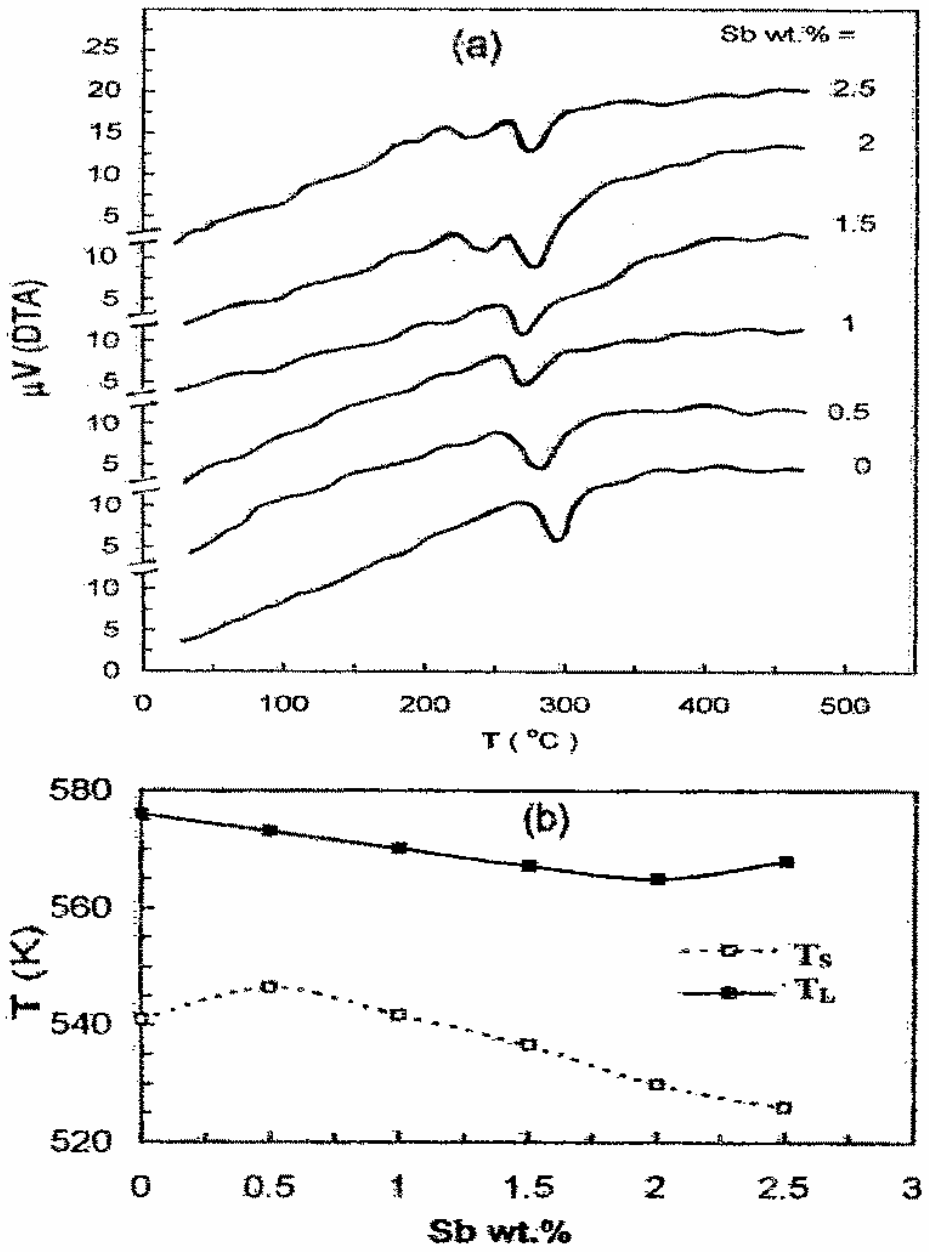

Fig. (3): (a) Thermograms of the binary ($PbSn_{12}$) and ternary alloys (with Sb wt.% additions as indicated) with heating rate of 10 °C/min and b) The temperature variations of the endset (liquidus, T_L) and the onset (solidus, T_S) with increasing Sb content.

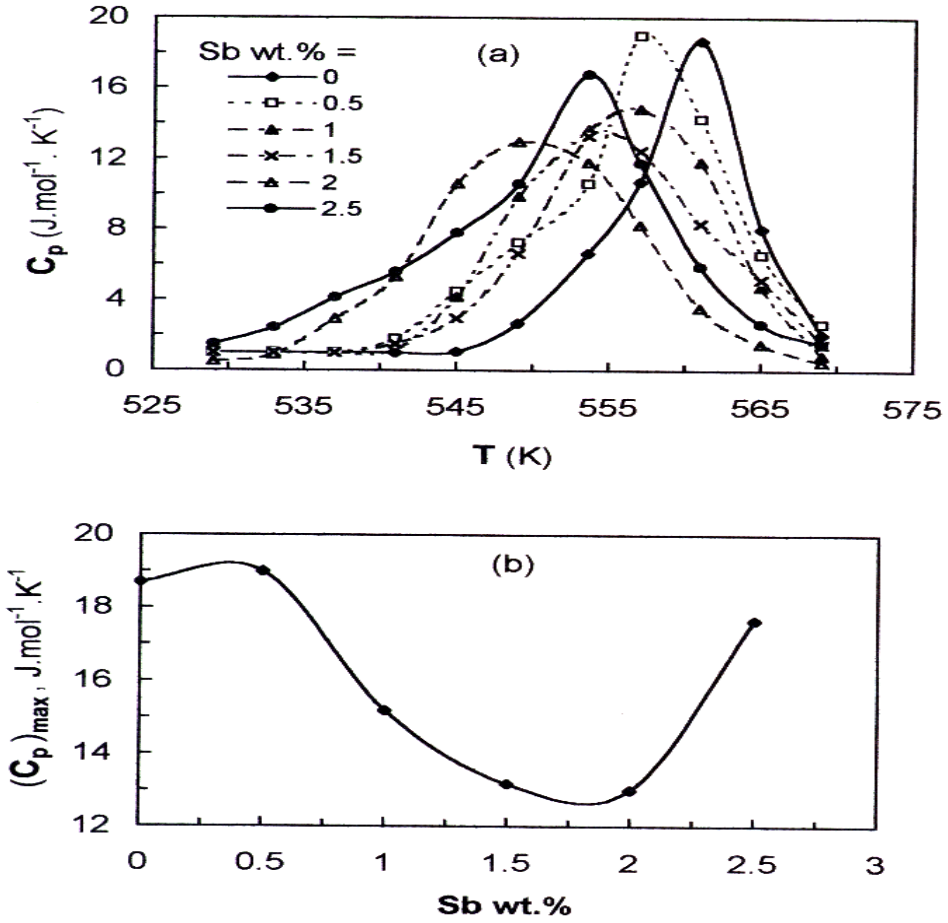

Fig. (4): a) Temperature dependence of the specific heat of the investigated $PbSn_{12}$ melt-spun alloy samples at different additions of Sb wt.% and b) The maximum value of specific heat $(C_p)_{max}$ as a function of Sb content

The excess specific heat ΔC_p obeys the experimental low [31],

$$\Delta C_p = A\,(NU^2/RT^2)\exp(-U/RT) \qquad (5)$$

where **N** is the number of atoms displaced from the equilibrium position, **U** is the activation energy of the thermally activated ordering, **R** is the universal gas constant and **A** is the coordination number. Using equation 5, the relation between ln ($\Delta C_p T^2$) and 1000/T yields straight lines for all the tested samples as shown in Fig. (5a). The Sb concentration dependence of the activation energy obtained from the slopes of the lines of Fig.(5a) is given in Fig.(5b). From Fig.(4b), the behaviour of $(C_p)_{max}$ seems to be inversely related to **U** for Sb content above 1 wt.%.

The microstructure produced by rapid solidification may be a direct result of the solidification process, or caused by a post-solidification coarsening. The melting point of Pb-Sn alloy is not very much above room temperature and rapid coarsening has been observed in degenerate wavy lamellar microstructure [32]. The coarsening rate can be enhanced either by the presence of primary dendrites or by deformation produced by the shearing effect of the liquid flow during melt spinning. Also, a metastable hexagonal phase forms when the Pb-Sn alloy is quenched to low temperatures [1].

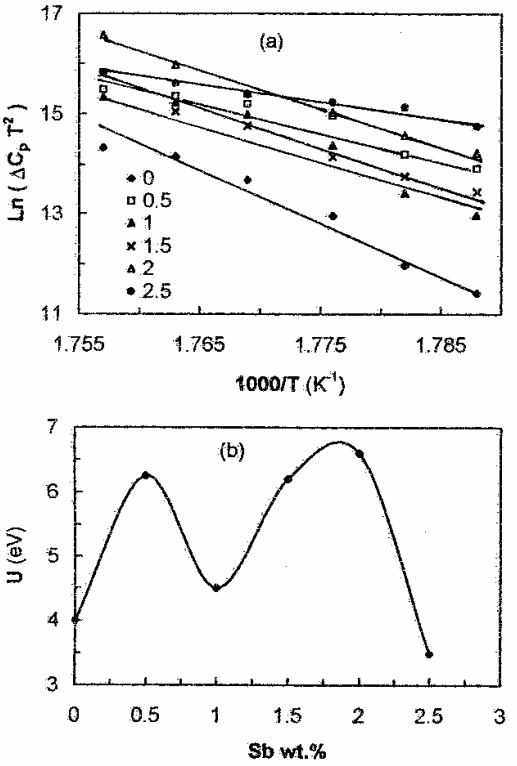

Fig. (5): a) The ln (ΔC_p T^2) values against 1000/T at different additions of Sb wt.% and b) The Sb concentration dependence of the activation energy (U).

By heating the rapidly solidified Pb- rich phase, (α-phase), the Sn- rich phase, (β-phase) starts to form due to a solution process at some of the interfaces and to a precipitation process at other ones through diffusion process [22]. The supersaturated pb-rich phase is therefore transformed to the stable binary Pb- rich and Sn- rich phases. Below 393K these phases coarsen [22] and the mutual solubility increases to approach the actual equilibrium composition at each testing temperature. The precipitated Sn atoms cause increased strength [23]. Further heating near the solidus line causes the previously precipitated Sn atoms to dissolve. The directional movements of atoms give rise to dynamic recovery. This leads to increased density of mobile dislocations [23] and hence a decrease in strength is observed. The variations observed in the measured parameters are therefore mainly due to these structural variations. From the obtained data, Sb seems to intensify the behaviours observed with the binary alloy.

A representative example for the variation of $\Delta R_t/R_o$ as a function of precipitation time $\mathbf{t_p}$ at different precipitation temperatures $\mathbf{T_p}$ is given in Fig.(6a) for the binary and the ternary tested alloys with 0.5 and 2.5 wt.% Sb. Resistivity as a structure sensitive property, substantiates that the reaction

kinetics determined by resistivity are truly representative of the DP rate in the tested alloys. The reaction rates in the ternary alloys are considerably lower than that in the binary Pb-Sn alloy at all the tested precipitation temperatures. The reduction in precipitation kinetics assumes a significant proportion with the progress of reaction.

The atomic diameters of Sn and Sb are nearly equal but much smaller than that of Pb around room temperature [33]. Therefore, the matrix strain due to atomic size difference of Sb compared with the binary alloy may be negligible. Also, the bulk diffusion rate of Sb is two and three orders of magnitude larger than that of Pb and Sn, respectively in Pb matrix [33]. Hence, redistribution of Sb through the migrating reaction front (RF) during DP in the ternary alloys is unlikely to be the slowest step of the precipitation process. Moreover, Sb additions caused positive deviation in the valence electron difference with respect to the solute- solvent valence electron difference in the binary alloy. Therefore, it is suggested that neither the solute- solvent atomic size mismatch factor nor the change in valance electron difference could account for the observed reduction in the DP kinetics due to Sb additions to the Pb-Sn alloy.

Figure (6b) provides a direct comparison of the extent of the DP reaction in terms of the factor $\Delta R_f/R_o$ as a function of T_p. It is clear that the effect of ternary addition is more pronounced at lower T_p. The highest temperature T_{DP} for DP process in these alloys, as derived by extrapolating $\Delta R_f/R_o$ to $\Delta R_f/R_o$ =0, as shown in Fig. (6b), is essentially the same for both binary and the ternary alloys. Apparently, the DP reaction mechanism remains unaltered in the ternary alloys despite the considerable reduction in the growth kinetics due to Sb addition. It is significant that the incubation period remains effectively the same for the tested alloys such that the DP initiates at similar instances of time in both the

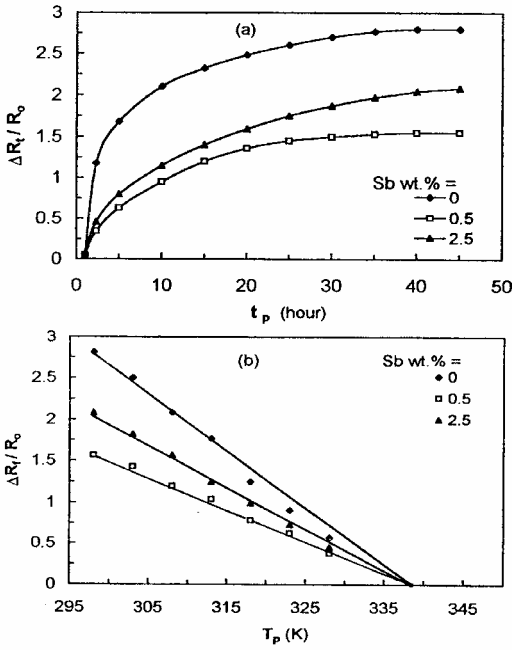

Fig. (6) A representative example for the variation of $\Delta R_f/R_o$ as a function of: precipitation time, t_p precipitation temperature, T_p. For the binary and the ternary tested alloys with 0.5 and 2.5Sbwt.%.

binary and ternary alloys as shown in Fig.(6b). This suggests that the effect of Sb appears to be confined mainly to the growth rather than to the nucleation stage of the reaction.

The effect of Sb on DP kinetics can be explained by a mechanism involving gradual adsorption of the impurity atoms at the moving RF as it sweeps through the untransformed matrix. Under such condition, the RF moves at a rate at which the solute atmosphere can migrate [20].

Representative examples of the X-rays diffraction patterns for the binary alloy, and the ternary alloy with 0.5 wt.%Sb are given in Fig. (7a, b), respectively. The analysis of these patterns indicates that the tested melt-spun ribbons exhibit broad diffuse peak typical of amorphous alloy. The amorphous metastable state is characterized by a random distribution of atoms. On the otherhand, Fig. (7b) for the melt-spun $PbSn_{12}Sb_{0.5}$ alloy is that of a crystalline state. This pattern indicates the formation of SnSb intermetallic compound identified by the planes (220) and (222) in Fig. (7b).

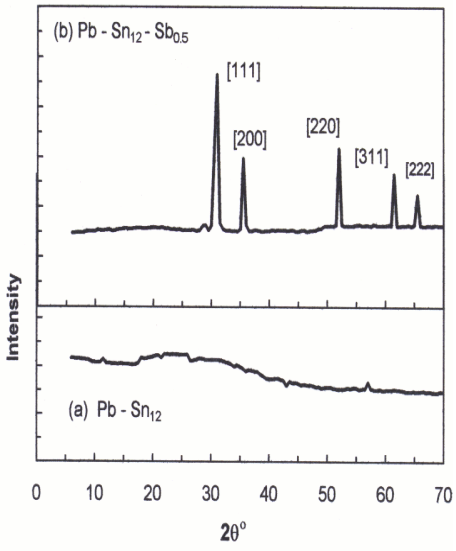

Fig. (7) XRD patterns of the melt-spun alloys: a) binary alloy ($PbSn_{12}$) and b) ternary alloy ($PbSn_{12}Sb_{0.5}$)

References

1. R.Cheese and B.Cantor, Mater. Sci. Eng. **45**, 83 (1980).
2. J.Liang, N.Gollhardt, P.S.Lee, S.A.Schroeder and W.L.Morris, Fatigue Fract. Engng. Mater. Struct. **19**, **11**, 1401 (1996).
3. M.Kamal, A.M.Shaban, M.El-kady and R.Shalaby, Radiation Effects and Defects in Solids, **138**, 307 (1996).
4. D..A.Gerord, Mater. Sci. Eng. A.Struct.Mater. **A 129**, 1 (1997).
5. M. McCormack, H.S.Chen, G.W.Kammalot, S.Jin, J. Electron Mater. (USA) 26, **8**, 954 (1997).
6. T.K.Ha and Y.W.Chang, Scripta Materialio, **37 (**9), 1415 (1997).
7. Q.Li, E.Johnson, A.Johansen and L.Sarholt-Kristensen, J.Mater. Res. 7, 2756 (1992)
8. B.Cantor (ed.), Proc. 3rd Int. Conf. On Rapidly Quenched Metals, Brighton, 1978, Metals Society London, (1978).
9. N.R.Green, J.A.Charles,G.C.Smith, Mater. Sci. Technol. (UK) **10**, 977 (1994).
10. M.Kamal, A.B.El-Bediwi and M.B.Karman, J. Mater. Sci. Materials in Electronics **9**, 425 (1998).

11. H.Johnes and C.Suryanarayana, J. Mater. Sci., **8**, 705 (1973).
12. G.Thomas and R.H.Willens, Acta Metall., **13**, 139 (1965), **14**, 138 (1966).
13. Y.Inokuti and B.Cantor, J. Mater. Sci., **12**, 946 (1979).
14. S.D.Felicelli, J.C.Heinrich, D.R.Poirier, Proceedings Supercomputing 92 (Cat. No. 92 CH3216-9), Minneapolis, MN, US, p. 433 (Nov. 1992).
15. S.N.Tewari, and R.Shah, Metall. Trans.A, Phys. Metall. Mater. Sci. (USA) **23A**, 12, 3383 (1992).
16. Y.Ma and T.G.Langdon, Metall. Trans. **25A**, 2309 (1994).
17. T.K.Ha, H.C.Shin, Y.W.Chang, J.Korean Inst. Met. Mater. **35**, 191 (1997).
18. P.Zhang, Q.P.Kong and H.Zhou, Phil. Mag. A Phys. Condens. Matter. Struct. Defects Mech. Prop. (UK), 77 (2), 437 (1998).
19. R. Alarashi, A.M.Shaban and M.Kamal, Materials Letters **31**, 61 (1997).
20. I.Manna and S.K.Pabi, Phys. Stat. Sol. (a) **123**, 393 (1991).
21. M.M.El-Sayed, R.Abd El-Haseeb, F.Abd El-Salam and M.R.Nagy; phys. stat. sol. (a) **143**, K83 (1994).
22. M.M.El-Sayed, F.Abd El-Salam, R.Abd El-Haseeb and M.R.Nagy; phys. stat. sol. (a) **144**, 329 (1994).
23. M.M.El-Sayed, F.Abd El-Salam and R.Abd El-Haseeb; phys. stat. sol. (a) **147**, 401 (1995).
24. M.Kamal, A.M.Shaban, M. El-Kady, A.M.Daoud and R.Alarashi, U.Scientist Phys. Sciences, **8**, (2), 166 (1996).
25. S.H.Liu, D.R.Poirier, P.N.Ocansey; Metall. Mater. Trans. A, Phys. Mater. Sci. (U.S.A), **26 (A),** 741 (1995).
26. A.M.Shaban and M.Kamal; Radiation Effects and Defects in Solids, **133**, 5 (1995).
27. J.L.Davis, Wave Propagation in Solids and Fluids (Springer- Verlag, New York) Chap. 8 (1988).
28. R.H.Nada, A.M.Abd El-Khalek and F.Abd El-Salam; "Fifth Radiation Physics Conference (RPC-2000)", Egypt. Soc. Nucl. Sci.& Applications. (ESNSA), 34 (1), 59 (2001).
29. A.Y.Malkin, A.A.Askadsky, V.V.Kovriga, and A.E.Chalykh, Experimental Methods of Polymer Physics, Mir Publishers, Moscow, p. 213 (1983)
30. T.N.El-Ashram, M.Sc. Thesis, Faculty of Science, Mansoura Univ., Mansoura, p. 63 (1996).
31. V.P.Burtsera, S.E.Vasil and U.M.Varirash, Sov. Phys. Sol. Stat., **30**, 877 (1988).
32. J.D.Verhoeven, D.P.Mower and E.D.Gibson, Metall. Trans. A, **8**,1239 (1977).
33. C.J.Smithhells and E.A.Brandes (Eds.), Metals Reference Book, Butterworth, London (1976).